www.czasopisma.pan.pl PAN POLSKA AKADEMIA NAUK www.journals.pan.pl

Arch. Metall. Mater. **65** (2020), 2, 911-916

DOI: 10.24425/amm.2020.132838

D. CZEKAJ[1], A. LISIŃSKA-CZEKAJ[1], K. KRZYSZTOFOWICZ[1*]

INFLUENCE OF CERAMIC COATING ON MECHANICAL PROPERTIES OF STAINLESS STEEL

Crystal structure and phase composition of stainless steel substrates (AISI 304 type) was studied and it was found that they adopted the cubic symmetry. The calculated elementary cell parameter for the mayor Fe-Ni phase (weight fraction 99%) was a = 3.593 Å, whereas the mean grain size was $\langle D \rangle$ = 2932 Å. Morphology of the stainless steel substrate surface was studied with profilometry. Mechanical properties of the stainless steel substrates and stainless steel substrates coated with ceramic layer of barium strontium titanate were studied with microhardness tester. For measurements performed according to the Vickers method the average microhardness was found HV = 189 or HV = 186 for the "in-line" and "mapping" measurement pattern, respectively. The sol-gel method was used to coat the surface of the stainless steel substrate with a thin ceramic layer of the chemical composition $Ba_{0.6}Sr_{0.4}TiO_3$. It was found that the stainless steel substrate covered with sol-gel deposited ceramic coating exhibited the average hardness within the range HV = 217 up to HV = 235 for loading force F = 98 mN and F = 0.98 N, respectively. The Knopp method was also used and it was found that the stainless steel substrate with $Ba_{0.6}Sr_{0.}4TiO_3$ coating exhibited hardness HK = 386.

Keywords: stainless steel, X-ray analysis, microhardness, sol-gel ceramic coating

1. Introduction

Stainless steels are materials whose importance is growing every year, due to their exceptional properties [1]. They are materials that contain iron, carbon, chromium and nickel. Chromium (Cr), which is added in at least 10.5% by weight, is responsible for the improved corrosion resistance of the alloys. The surface reaction of stainless steel with oxygen in the air creates a "passive" layer that almost eliminates environment-dependent corrosion, if it is continuous and does not get damaged.

Stainless steel exhibits three main types of microstructure, namely: ferritic, austenitic and martensitic. Its microstructure depends mainly on the chemical composition. Stainless steel could be categorized in several main classes [2], with minimum properties requirements described in the standards e.g. EN 10088.

The special properties of stainless steel mean that they can be used as substrates with various geometric shapes for applying coatings. Such coatings can not only improve the corrosion resistance of steel in a variety of aggressive environments, but also act as functional coatings that exhibit properties that cover industrial purposes and meet very specific demands and find unique applications [3]. For example, they can be used in biomedical applications for protection of orthopaedic implants, or improvement of the resistance to wear and tribological properties [4,5].

One of the methods of characterization of metallic material is a hardness measurement. The hardness test has the advantage of being non-destructive, so strength can be measured without destroying the component, and it requires only a tiny volume of material. But the information it provides is less accurate and less complete than the tensile test, so it is not used to provide critical design data. However, based on hardness data one can estimate the influence of the processing conditions (time, temperature applied) on the steel substrate properties. Among the hardness measurement methods one can mention the Vickers and Knoop hardness test methods [6,7] as the most usable for thin films and thin substrates characterization.

In the Vickers hardness test method the diamond square-based pyramid is loaded on the flat surface with the specific force and the indentation is made. The hardness value (HV number) is determined by the ratio F/A, where F is the force applied [N] and A is the surface area of resulting indentation in square millimetres. Indentation area is estimated based on the indentation diagonals d [mm] with formula (Eq. (1)):

$$A \approx \frac{d^2}{1.8544} \tag{1}$$

[1] GDAŃSK UNIVERSITY OF TECHNOLOGY, FACULTY OF MECHANICAL ENGINEERING, DEPARTMENT OF MATERIALS ENGINEERING AND WELDING, 11/12, NARUTOWICZA STR., 80-233 GDAŃSK, POLAND

* Corresponding author: krzysztof.krzysztofowicz@pg.edu.pl

The hardness value is calculated base on the equation Eq. (2):

$$HV \approx 0.1891 \frac{F}{d^2} \tag{2}$$

The advantages of the Vickers hardness test are that extremely accurate readings can be taken, and just one type of indenter is used for all types of metals and surface treatments.

Goal of the present research was to study mechanical properties of stainless steel in terms of its microhardness as well as its microstructure, crystal structure and phase composition. Influence of sol-gel deposited ceramic coating on hardness of the stainless steel substrates is reported.

2. Experimental

Crystal structure of the AISI 304 type stainless steel substrates was studied by X-ray diffraction method at room temperature (Philips PW 3710 X-ray diffractometer, Θ – 2Θ mode, CoKa radiation, detector scan step Δ2Θ = 0.01° scan step time t = 8 s, scan type: continuous).

Phase analysis of X-ray diffraction patterns of stainless steel substrates was carried out using Match! (Crystal Impact) computer programme [8]. The structural analysis was performed with X'pert HighScore Plus software (PANalytical B.V). The latest available ICSD [9], ICDD [10] and IUCr/COD/AMCSD [11] databases were utilized. Refinement of the structural parameters of stainless steel substrates was performed with the Rietveld method [12].

Taylor Hobson Talysurf-type profilometer was used for examination of the geometric structure of the surface of the stainless steel substrates.

Microhardness measurements of the stainless steel substrates both polished and coated with ceramic film of the chemical composition $Ba_{0.6}Sr_{0.4}TiO_3$ (BST6040) were performed with fully automatic microhardness testing system FM-ARS9000-type (Future-Tech Corp.). Visualization and calculations were performed with a program module for processing and analysis of measured data FT-ARS Ver. 1.16.2. (Future-Tech Corp) [13].

BST6040 ceramic coating was applied on polished stainless steel substrates by sol-gel spin-coating technique. In today's terminology, sol-gel processing is a form of nanostructure processing [14]. Not only does the sol-gel process begin with a nanometre-sized unit, a molecule, it also undergoes reactions on the nanometre scale resulting in a material with nanometre features [15].

In the present study, barium acetate ($Ba(CH_3COO)_2$, 99%), strontium acetate ($Sr(CH_3COO)_2$, 99%), and tetra-butyl titanate ($Ti(OC_4H_9)_4$, 97%) were used as starting materials. Glacial acetic acid (CH_3COOH) as well as n – butanol ($CH_3(CH_2)_3OH$) were used as solvents. Acetyloacetone ($CH_3COCH_2COCH_3$) was added as stabilizer and water was used to complete a hydrolysis reaction. All above reagents were of analytic purity.

After stoichiometrically dissolved, mixed and stirred the precursor solution was deposited by spin coating on polished stainless steel substrates. Spin coating was performed at ω = 3500 revolution per min for t = 30 s to form wet films. The coating process was repeated up to 15 times thus yielding thin films of d = 300 nm in thickness. Final crystallization of as-deposited BST thin films was carried out in an ambient atmosphere at T = 600°C-800°C for t = 2 hours (the heating rate was 2°C/min) by conventional furnace annealing.

3. Results and discussion

3.1. Crystal structure and phase composition

An example of X-ray diffraction pattern of AISI-304 – type stainless steel recorded at room temperature is shown in Fig. 1. The search-match procedure was performed after raw data processing. The visual inspection of the diffraction data given in Fig. 1 have shown that there are three strongest diffraction lines at 2Θ ~ 51°, 59° and 89°. There are also less intense diffraction lines visible in the diffraction pattern at the angle 2Θ ~ 52°, 77° and 99°.

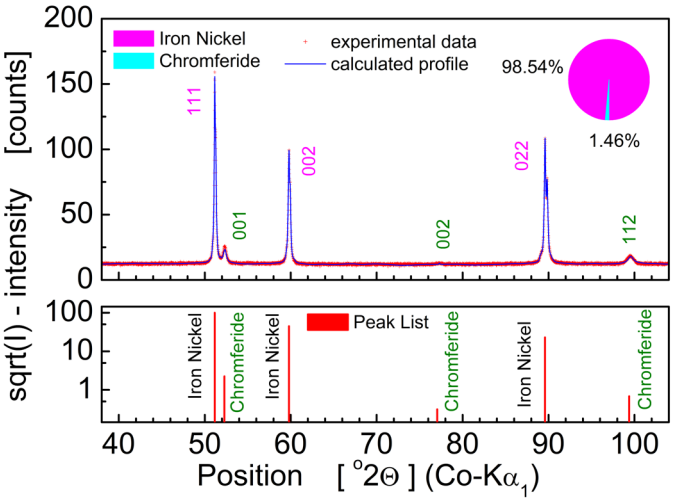

Fig. 1. Results of the X-ray pattern fitting for stainless steel substrate. Crosses (red) – experimental points; line (blue) – refined structure. Bottom plot shows identification of the phases of the stainless steel substrate

The detailed X-ray phase analysis showed that the experimental diffraction peaks match two phases, namely the iron nickel phase of the chemical composition $Fe_{2.6}Ni_{1.4}$, and chromferide phase with the chemical composition $Cr_{0.053}Fe_{0.947}$ (see bottom plot in Fig. 1).

The detailed structural analysis of was performed with Rietveld method. A model structure of iron nickel phase (cubic symmetry, *Fm-3m* (No. 225) space group) according to the ICSD database (code 632924) and chromferide phase (cubic symmetry, *Im-3m* (No. 229) space group) according to ICSD database (code 102753) were taken as initial structures for structural parameters refinement.

Results of the detailed X-ray structural and phase analysis are given in Fig. 1. It should be noted that the calculations were

performed for XRD profile modelled with a Pseudo-Voigt function. The following *R*-parameters (quality of the fitting) were obtained: R_p = 18.14%, R_{wp} = 24.36%, R_{exp} = 7.79%. Calculated density of iron nickel was ρ = 8.14 g/cm^3 and calculated elementary cell parameter was a = 3.593 Å. Calculated density of chromferide was ρ = 7.77 g/cm^3 and calculated elementary cell parameter was a = 2.875 Å. Crystallite size was found as follows: for iron nickel phase $<D>$ = 2932 Å and for chromferide phase $<D>$ = 32414 Å, respectively.

3.2. Stereometrical characterization of stainless steel substrates

The polished stainless steel of AISI 304-type substrates were also characterized from the stereometrical point of view. Taylor Hobson Talysurf-type profilometer was used for examination of the geometric structure of the surface. Results are given in Fig. 2, Fig. 3. and table Table 1.

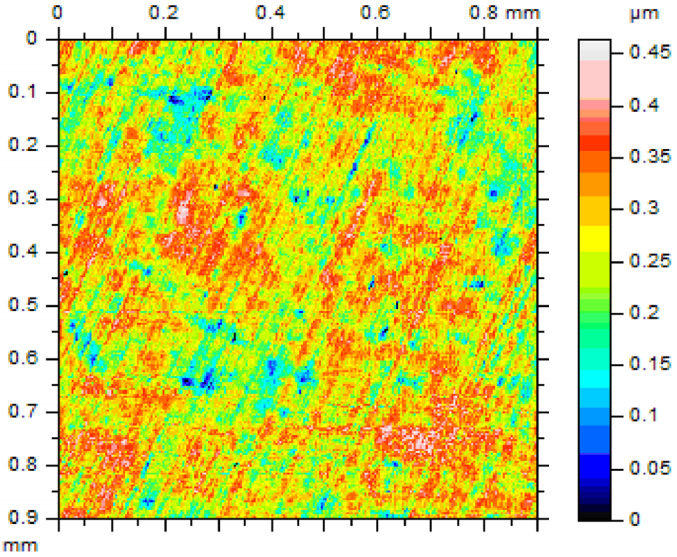

Fig. 2. Intensity colour map of the surface of the stainless steel substrate

TABLE 1

Stereometrical parameters of the stainless steel substrate

Parameter		Value
Sp – Maximum height of peaks;	[µm]	0.192
Sv – Maximum height of valleys;	[µm]	0.272
Sz – Maximum height of the surface;	[µm]	0.4
Sa – Arithmetic mean height of the surface;	[µm]	0.05

3.3. Microhardness of stainless steel substrates

Hardness of the stainless steel substrates was measured using the Vickers method, according to EN-ISO 6507-1:2018. To perform the measurements the force of F = 0.98 N was applied due to low thickness of the stainless steel substrate. Two measurement patterns were applied (Fig. 4). First the 10 indents in-line were made, next the matrix of 5×5 indents was made. The measurements were taken in places distant from each other.

In case of the stainless-steel substrate with ceramic coating the similar pattern was applied concerning the in-line measurement. Apart from the Vickers method the Knoop method was also applied to evaluate hardness. Results of the measurements are presented in Fig. 5-9.

One can see from Fig. 4a and Fig. 5a that the obtained indentation points for stainless steel substrate were regular and, in some cases, small plastic deformation of substrate material close to indentation point was observed (Fig. 4a, Fig. 5a). Similar situation occurred in case of the indentation matrix for the stainless steel substrate (Fig. 4c).

In case of the ceramic-coated stainless steel substrate indentations were also clearly visible (Fig. 4b). Small deformation were observed under higher magnification (Fig. 5b). On the other hand, Knoop indentations shown in Fig. 5c, caused larger deformation of the surface.

Results of the hardness measurements performed according to the Vickers method at loading force F = 0.98 N for stainless steel substrate are given in Fig. 6 and Fig. 7.

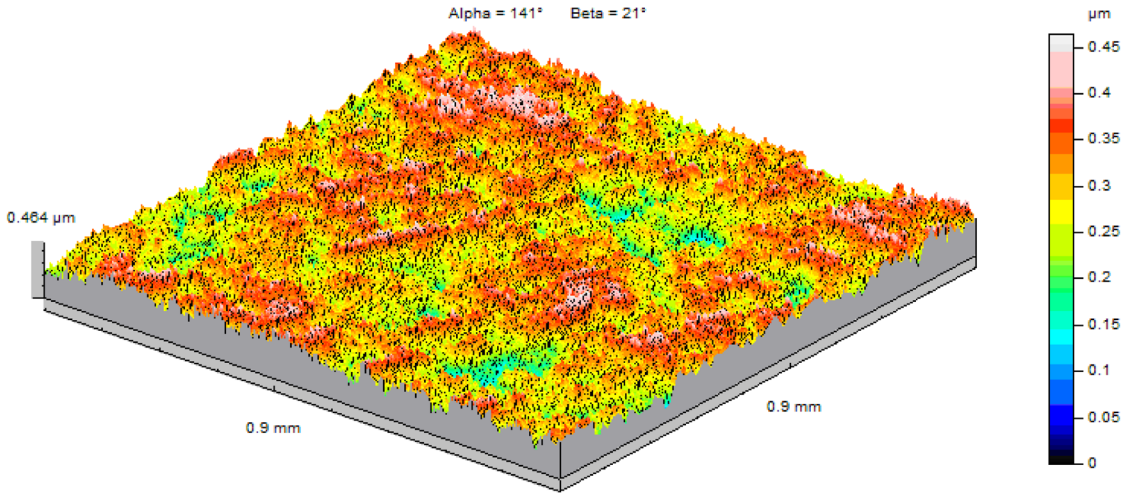

Fig. 3. Isometric picture (3D) of the surface of the stainless steel substrate

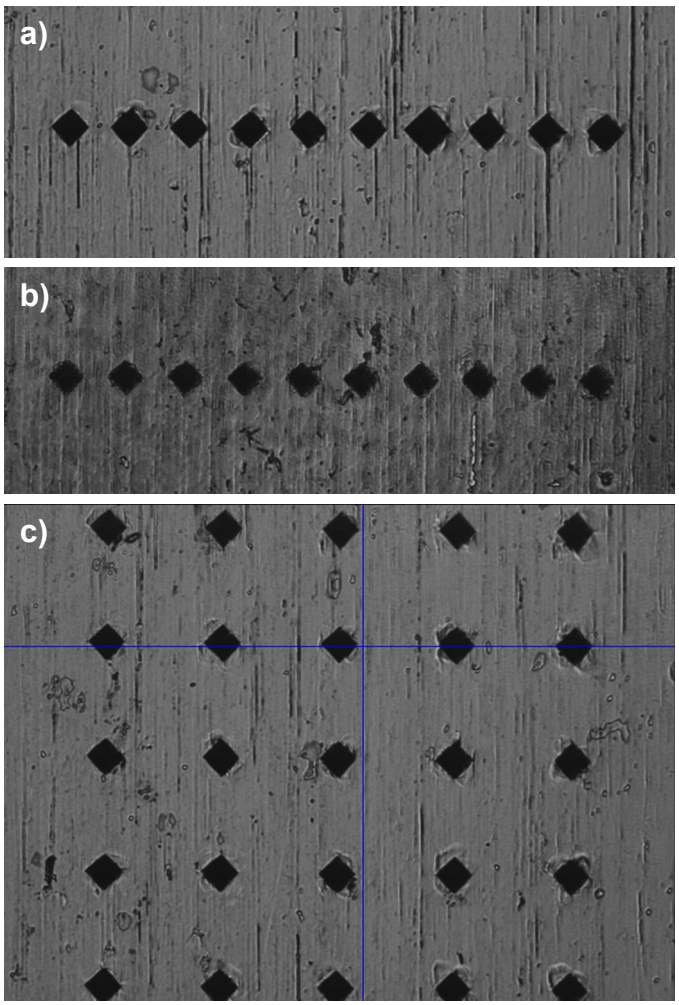

Fig. 4. Measurement patterns used for the Vickers hardness tests. (*a*) – "in-line" indentation pattern used for characterization of the stainless steel substrates; (*b*) – "in-line" indentation pattern used for ceramic-coated stainless steel characterization; (*c*) – "matrix" indentation measurement pattern used for characterization of the stainless steel substrates

One can see from Fig. 6 that microhardness measured according to the "in-line" measurement pattern (Fig. 4a) exhibited some irregularities. Variation in mechanical properties across stainless steel surface was studied due to mapping (the "matrix" measurement pattern – Fig. 4c) and the distribution of microhardness is shown in Fig. 7.

It was found however, that mean value of microhardness calculated on the base of "in-line" measurements was $HV = 189$ whereas mean value of hardness calculated on the base of "mapping-type" measurements was $HV = 186$.

3.4. Influence of ceramic coating on microhardness of stainless steel substrates

The thin film ceramic coatings of the chemical composition $Ba_{0.6}Sr_{0.4}TiO_3$ were deposited on the stainless steel substrate after a thorough cleaning process including ultrasonic and wet chemical cleaning. Many previous investigations have focused

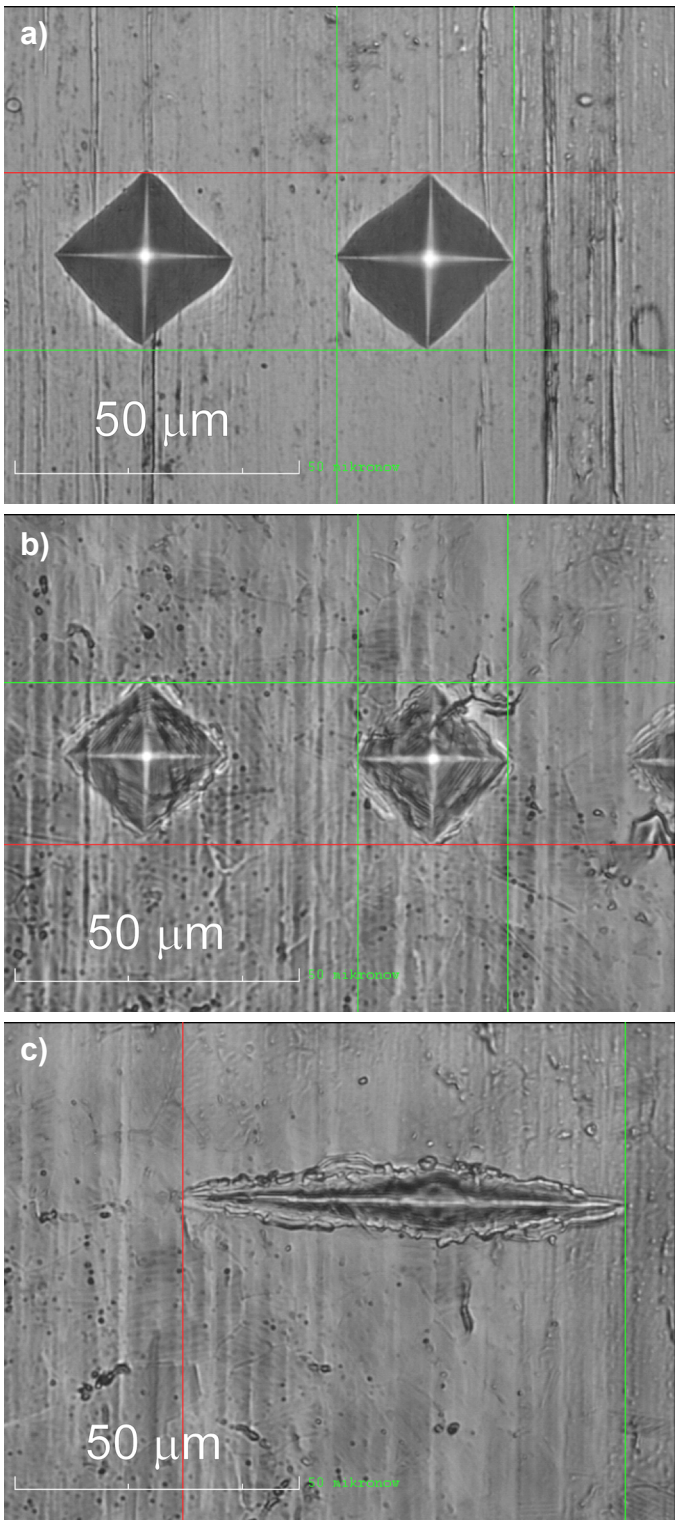

Fig. 5. Images showing the indents made at the loading force $F = 0.98$ N. (*a*) – shape of the indents made on stainless steel surface according to the Vickers hardness test; (*b*) – shape of the indents made on ceramic-coated stainless steel according to the Vickers hardness test; (*c*) – shape of the indents made on ceramic-coated stainless steel according to the Knopp hardness test

on fabricating barium strontium titanate thin films on the conventional $Pt/Ti/SiO_2/Si$ substrates. Stainless steel substrates exhibit their advantages in low cost, integrating thin films with devices for the MEMS-structure tuneable microwave devices. However,

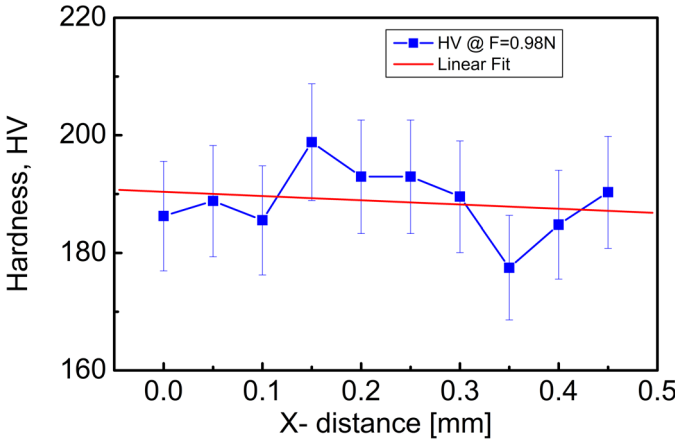

Fig. 6. Results of hardness measurement for the stainless steel substrate performed according to the Vickers method at loading force $F = 0.98$ N

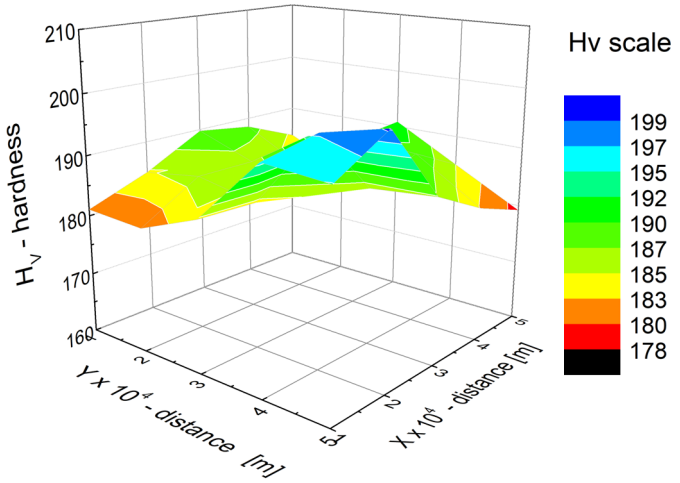

Fig. 7. Distribution of microhardness on the surface of the stainless steel substrate (the Vickers hardness test, the loading force $F = 0.98$ N)

when stainless steel is used as a substrate, lattice misfit stress, thermal stress, and even the inter-diffusion between films and substrates are accordingly accompanied, which would produce many defects and have disadvantages for crystal growth and dielectric properties of thin films [16].

Properties of the nanostructured BST6040 thin film ceramic coatings of the deposited on stainless steel substrates by sol-gel spin coating technique have already been reported in scientific journals. The studies were focused on crystal structure and dielectric properties [17], microstructure and piezoelectric properties in nanoscale [18], nanomechanical properties [19], or optical properties BST thin films [20].

In case of object of investigation consisting of stainless steel substrate coated with $Ba_{0.6}Sr_{0.4}TiO_3$ ceramic thin layer the measurements were performed under application of the loading force of $F = 0.98$ N and $F = 98$ mN. One can see from Fig. 8 that in both cases the hardness measurements performed according to the Vickers method for the stainless steel substrate with BST6040 ceramic coating showed an increase in the value of hardness in comparison to the uncoated stainless steel substrate (Fig. 6, Fig. 7). The average hardness value was found as follows: HV = 235 for $F = 0.98$ N and HV = 217 for $F = 98$ mN. The higher the loading force F the higher value of the average hardness HV was found.

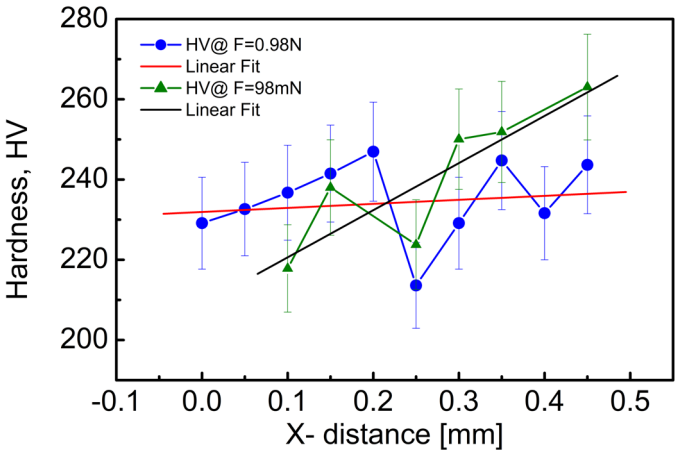

Fig. 8. Results of the Vickers hardness test of the ceramic-coated stainless steel substrate performed at the loading force $F = 0.98$ N (circles) and $F = 98$ mN (triangles)

In case of the ceramic-coated stainless steel substrate the Knopp indenter was also used [7] and the results of hardness measurements at the loading force $F = 98$ mN are shown in Fig. 9.

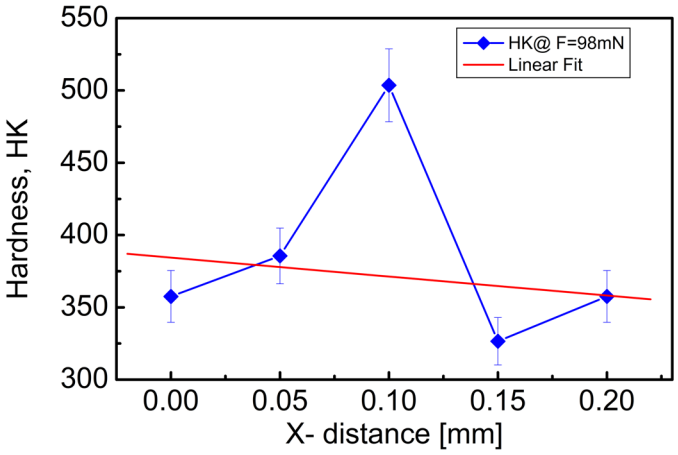

Fig. 9. Results of the Knopp hardness test of the ceramic-coated stainless steel substrate performed at the loading force $F = 98$ mN

It is worth noting that in case of the measurement according to the Knoop method the average hardness value was $HK = 386$. It should be pointed out that the values obtained are significantly higher than those obtained for Vickers measurement method under same loading force applied. That requires the future investigation.

4. Conclusions

X-ray diffraction analysis followed by the Rietveld refinement method made it possible to find that stainless steel substrate consisted of iron nickel phase (weight fraction 98.54%) and

chromferide phase (weight fraction 1.46%). The major phase (i.e. iron nickel, $Fe_{2.6}Ni_{1.4}$ phase) exhibited the cubic crystal structure described as *Fm-3m*(225) with an elementary cell parameter $a = 3.593$ Å and the mean grain size $\langle D \rangle = 2931$ Å. Statistical analysis of the stainless steel substrate surface roughness showed that average roughness is characterized with a parameter Sa = 50 nm.

Results of investigation of mechanical properties of the stainless steel substrates shown that they exhibited the hardness on the level of $HV = 189$ in case of in-line measurement pattern and $HV = 186$ in case of the matrix pattern of measurements. The results are very close one to another. In case of the stainless steel substrate with BST6040 ceramic coating the average hardness was found to be from 17% to 26% higher, namely $HV = 217$ or $HV = 235$ (depending on the loading force applied during Vickers measurements). Also an increased value of hardness was observed for Knoop hardness measurements, namely $HK = 386$. That confirms the substantial increase of stainless steel hardness after applying the sol-gel coating process.

Acknowledgement

The Authors are grateful for financial support according to financial grant no. 033827 provided by Gdansk University of Technology.

REFERENCES

[1] K.H. Lo, C.H. Shek, J.K.L. Lai, Recent developments in stainless steels, Mater. Sci. Eng. **R 65**, 39-104 (2009); DOI:10.1016/j.mser.2009.03.001.

[2] J. Beddoes, J.G. Parr, Introduction to Stainless Steels, 3rd edition, ASM International, Materials Park, OH, USA, (1999).

[3] J. Bautista-Ruiz, A. Chaparro, J.J. Olaya, Characterization of the tribological properties of bismuth-titanate coatings synthesized by sol-gel on 316L stainless steel substrates, Tribol. Indust. **41** (3), 452-462 (2019), DOI: 10.24874/ti.2019.41.03.15.

[4] B. Tlili, A. Barkaoui, M. Walock, Tribology and wear resistance of the stainless steel. The sol-gel coating impact on the friction and damage, Trib. Intern. **102**, 348-354, (2016), DOI: 10.1016/j.triboint.2016.06.004.

[5] H. Cheraghi, M. Shahmiri, Z. Sadeghian, Corrosion behavior of TiO_2-NiO nanocomposite thin films on AISI 316L stainless steel prepared by sol–gel method, Thin Sol. Fil. **552**, 289-296 (2012), DOI: 10.1016/j.tsf.2012.07.125.

[6] ISO 6507-1:2018 Metallic materials – Vickers hardness test – Part 1: Test method.

[7] ISO 4545-1:2017 Metallic materials – Knoop hardness test – Part 1: Test method.

[8] MATCH! Version 2.0.11, CRYSTAL IMPACT, Postfach 1251, 53002 Bonn, Germany (URL: http://www.crystalimpact.com/match).

[9] ISCD Database, FIZ Karlsruhe, (URL: http://www.fiz-karlsruhe.de)

[10] International Centre for Diffraction Data, 12 Campus Boulevard, Newton Square, PA 19073-3273 U.S.A.; (URL: http://www.icdd.com).

[11] IUCr/COD/AMCSD Database (URL: http://www.crystalimpact.com.match).

[12] H.M. Rietveld, The Rietveld method-a historical perspective, Austr. J. Phys. **41**, 113-116 (1988).

[13] Catalogue: https://www.ft-hardness.com/en/product/pdf/hardnesstester_ars01.pdf (source: URL: https://www.ft-hardness.com/en/index.html).

[14] L.C. Klein, Sol gel formation and deposition, In: A.N. Goldstein (Ed.), Handbook of nanophase materials, Marcel Dekker Inc., New York (1997).

[15] K. Kumar, K. Keizer, A. Burggraaf, T. Okubo, H. Nagamoto, S.Morooka, Densification of nanostructured titania assisted by a phase transformation. Nature **358**, 48-51 (1992). https://doi.org/10.1038/358048a0.

[16] H. Dong, G. Lu, D. Chen, D. Jin, J. Chen, J. Cheng, Effects of $LaNiO_3$ buffer layer on improving the dielectric properties of barium strontium titanate thin films on stainless steel substrates, J. Sol-Gel Sci. Technol. **80**, 848-852 (2016); DOI 10.1007/s10971-016-4169-y.

[17] D. Czekaj, A. Lisińska-Czekaj, T. Orkisz, J. Orkisz, G. Smalarz, Impedance spectroscopic studies of sol-gel derived barium strontium titanate thin films, J. Europ. Ceram. Soc. **30**, 465-470 (2010).

[18] D. Czekaj, A. Lisińska-Czekaj, J. Plewa, Study of nanomechanical properties of (1-y)BST-yMgO thin films, Ciên. Tecn. Mater. **29**, e71-e75 (2017).

[19] D. Czekaj, A. Lisińska-Czekaj, Piezoresponse force microscopy and dielectric spectroscopy study of $Ba_{0.6}Sr_{0.4}TiO_3$ thin films, J. Adv. Diel. **9** (3), 1950025 (2019), DOI: 10.1142/S2010135X19500255.

[20] D. Czekaj, A. Lisińska-Czekaj, Influence of Mg-doping on synthesis of sol-gel derived BST thin films, J. Adv. Diel. **2** (1), 1250010 (2012), DOI: 10.1142/S2010135X12500105.